Metabolic flux network analysis of hydrogen production from crude glycerol by *Clostridium pasteurianum*

Shyamali Sarma, Avinash Anand, Vikash Kumar Dubey, Vijayanand S. Moholkar

PII: S0960-8524(17)30450-9
DOI: http://dx.doi.org/10.1016/j.biortech.2017.03.168
Reference: BITE 17872

To appear in: *Bioresource Technology*

Received Date: 30 January 2017
Revised Date: 25 March 2017
Accepted Date: 27 March 2017

Please cite this article as: Sarma, S., Anand, A., Dubey, V.K., Moholkar, V.S., Metabolic flux network analysis of hydrogen production from crude glycerol by *Clostridium pasteurianum*, *Bioresource Technology* (2017), doi: http://dx.doi.org/10.1016/j.biortech.2017.03.168

Metabolic flux network analysis of hydrogen production from crude glycerol by *Clostridium pasteurianum*

Shyamali Sarma,[1] Avinash Anand,[2] Vikash Kumar Dubey,[3] Vijayanand S. Moholkar[1,2*]

[1] Centre for Energy, [2] Department of Chemical Engineering, [3.]Department of Biosciences and Bioengineering, Indian Institute of Technology Guwahati, Guwahati – 781 039, Assam, India

* Corresponding author. Tel: +91 9954709058, Fax: +91 361258 2291, E–mail: vmoholkar@iitg.ernet.in

ABSTRACT

The present study has attempted to get insight into ultrasound induced enhancement in biohydrogen production from glycerol fermentation using metabolic flux analysis (MFA). A pseudo steady state metabolic flux network model was constructed and analyzed using experimentally measured glycerol uptake rate and fluxes of four metabolites, viz. acetate, butyrate, succinate and 1,3–PDO. Glycerol consumption increased by ~50% under sonication. Biohydrogen yield showed marked rise of ~40% with application of ultrasound. Butyrate and 1,3–PDO were the major products of glycerol metabolism. Sonication had major influence on carbon fluxes at the acetyl–CoA node. MFA results revealed enhanced flux towards butyrate under sonication, which was manifested in higher butyrate to acetate (B/A) ratio in products and greater H_2 generation. Biohydrogen production was also a microbial growth associated process. Finally, two theoretical alternatives for further enhancement of biohydrogen production were assessed with MFA, viz. enhancement of glycerol uptake and blocking of butyrate pathway.

Keywords: Biohydrogen, Metabolic flux analysis, Glycerol, Fermentation, Butyrate to acetate ratio

1. Introduction

Biohydrogen has emerged as a potential alternate and clean fuel in recent years. Conventionally, hydrogen is produced on commercial scale by steam reforming of methane, which is highly energy intensive process. Fermentative production of hydrogen (popularly known as biohydrogen) is a potential solution to this issue. Among the biochemical routes for hydrogen production, dark fermentation presents a promising method due to the substrate flexibility and higher hydrogen yield (Guo et al., 2010; Argun et al., 2011; Ghimire et al., 2015; Urbaniec et al., 2015). Economic substrates in the form of lignocellulosic biomasses for dark fermentation require significant pretreatment that adds to overall production cost. More recently, glycerol has been explored as alternate substrate for biohydrogen production (Sittijunda et al., 2012; Varrone et al., 2012). Substitution of lignocellulosic biomasses with glycerol as fermentation substrate has gained high relevance in recent years due to unprecedented growth of biodiesel industry (Jitrwung et al., 2011; Sittijunda et al., 2012; Mangayil et al., 2012, 2015). Transesterification process for biodiesel production yields glycerol as the side product. However, this glycerol is contaminated with alkali and alcohol, and hence, not useful for conventional applications such as cosmetics, food and pharmaceuticals. This glycerol can be effectively used as fermentation substrate for production of several value–added products (Dikshit and Moholkar, 2016; Khanna et al., 2012a, 2013a, 2013b, 2014). Significant literature has been published in recent past that reports glycerol–based biohydrogen production (for example Trchounian et al., 2015; Marone et al., 2015; Varrone et al., 2012; Sittijunda et al., 2012). In our previous paper (Sarma et al., 2016) we have presented an extensive review of literature on biohydrogen production from glycerol.

Fermentation processes are limited by slow kinetics. The kinetics of fermentation can be boosted by optimization of the process conditions (such as pH, temperature, agitation rate

etc.) or by use of recombinant or genetically engineered microbial cultures (Mu et al., 2009; Wang et al., 2008; Liu et al., 2008; Morimoto et al., 2005). Another effective means of enhancing the fermentation kinetics is application of ultrasound irradiation or sonication to fermentation mixture. Ultrasound and cavitation make energy available on extremely small temporal and spatial scales (Moholkar and Warmoskerken, 2003).The physical and chemical effects of ultrasound can boost fermentation kinetics through enhancement of cellular transport and inducing conformational changes in secondary structure of enzymes (Singh et al., 2015a, 2015b; Bhasarkar et al., 2015a, 2015b; Borah et al., 2016). In our previous work, we have demonstrated effective use of ultrasound in boosting glycerol fermentation to butanol and 1,3–propanediol (Khanna et al., 2012b, 2013c). The metabolic pathway of glycerol bioconversion by *Clostridium sp*. is well established and is depicted in Fig. 1. Glycerol metabolism has two phases, viz. acidogenesis and solventogenesis. The initials steps in glycerol bioconversion are formation of dihydroxyacetone (DHA) by enzyme glycerol dehydrogenase with further conversion of DHA to DHA phosphate and finally to pyruvate. Conversion of pyruvate yields lactic acid or acetyl–CoA and CO_2 through pyruvate–ferredoxin (Fd) oxidoreductase, which occurs simultaneously with reduction of ferredoxin (Fd). Reduction of Fd by enzyme hydrogenase results in formation of H_2. The end products of acetyl–CoA conversion are acetic and butyric acid. Thus, the H_2 production is associated with formation of end products like acetate, butyrate and lactate.

The actual H_2 yield from glycerol fermentation is, however, lesser than theoretical yield. This result is essentially attributed to formation of lactate and other solvent products. Thus, in order to achieve high H_2 yield, degree of engagement of various pathways in overall cellular functions and metabolic processes needs to be properly studied. In other words, quantification of the magnitude of pathway fluxes *in vivo* is essential for maximizing production of the valuable metabolites. The intracellular metabolic fluxes can be estimated using stoichiometric

reaction models and mass balances for the metabolites. Metabolic flux analysis (MFA) is an useful methodology for determination of the fluxes in metabolic pathways. MFA is also an effective tool for understanding cell physiology and regulation of metabolism in different microorganisms. To the best of our knowledge, no study has been published on metabolic flux analysis of glycerol fermentation by *C. pasteurianum*. In present study, we have addressed this important issue with focus on biohydrogen yield from glycerol fermentation. A review of the previous literature on MFA of biohydrogen production by various microbial strains is given in Table S.1 provided in supplementary material. The present study essentially aims at utilizing the experimentally measured fluxes of certain metabolites (under steady state conditions) to estimate the complete intracellular fluxes and identify robustness of branch points (or nodes) of anaerobic glycerol metabolism in *C. pasteurianum* using MFA. An *in silico* metabolic flux model has been formulated for this analysis that determines the complete intracellular fluxes of all metabolites from experimentally measured fluxes. Batch mode fermentation of glycerol has been carried out with mechanical shaking (control experiments) and sonication (test experiments) using pre–optimized conditions of pH, temperature and initial glycerol concentration (Sarma et al., 2016). Comparative analysis of the metabolic fluxes in the control experiments and ultrasound–assisted (or test) experiments has given insight into the influence of ultrasound on glycerol metabolism and H_2 yield.

2. Materials, methods and model

2.1. Microorganism and fermentation conditions

Microbial culture of *Clostridium pasteurianum* MTCC 116 (ATCC 6013) was procured from Microbial Type Culture Collection (MTCC), Chandigarh, India. Pure glycerol was procured from Merck, Germany. All other medium components and chemicals used in this study were procured from HiMedia Pvt. Ltd., India. The standards of acetic acid, butyric acid, lactic acid, succinic acid and1,3–PDO were of HPLC grade and procured from HiMedia

Pvt. Ltd., India.

Freeze dried cultures of *C. pasteurianum* were maintained in Reinforced Clostridial Medium (RCM). The composition of RCM in 1 L of distilled water was as follows: yeast extract 5.0 g, beef extract 10.0 g, peptone 10.0 g, glucose 5.0 g, starch 1.0 g, sodium chloride 5.0 g, sodium acetate 3.0 g, cysteine hydrochloride 0.5 g, agar 0.5 g. The pH of the medium was adjusted to 6.8 ± 0.2 using 1 M NaOH. The medium was inoculated and kept in a rotary incubator shaker (Make: Lab Companion; Model: SI–300R) at 37^{o}C, 150 rpm for 24 h. The 24 h culture was used for streaking over agar plate containing 15 g/L of agar in medium with same composition as stated above. The culture was kept at 37^{o}C in a desiccator containing anaerobic gas pack. The culture broth was used as stock and was sub–cultured every month.

The cells from stock culture were grown under anaerobic conditions in fresh RCM prior to inoculation. Batch fermentation experiments were set up in 100 mL serum bottles containing BSH medium at pre-optimized conditions (pH = 6.7, temperature = 36°C, crude glycerol concentration = 7.4 g/L) (Sarma et al., 2016). The total working volume of fermentation mixture was 50 mL with following composition: 5 mL (or 10% v/v) of *C. pasteurianum* inoculum (containing microbial cells in mid–log phase), 1 mL of 3% w/v L–cysteine HCl as a reducing agent, and 44 mL of fermentation medium (BSH) including substrate crude glycerol (7.4 g/L). The crude glycerol employed as fermentation substrate was produced in–house through alkali catalyzed methanolysis of soybean oil. This glycerol had contaminations of alkali (NaOH, 0.85% w/v) and alcohol (methanol, 0.26% w/v). The levels of these impurities were determined by either acid–base titration or gas chromatograph (Sarma et al., 2016). Resazurin dye (0.1% w/v) was added to fermentation medium as indicator of anaerobic conditions. The BSH medium comprised of following components (concentration, g/L): peptone (2), yeast extract (1), K_2HPO_4 (0.230), KH_2PO_4 (4.035), in addition to 10 mL trace solution and 10 mL vitamin solution. Trace element solution comprised of following

components (concentration, g/L): $MnO_4 \cdot 7H_2O$ (0.01), $ZnSO_4 \cdot 7H_2O$ (0.05), H_3BO_3 (0.01), $N(CH_2COOH)_3$ (4.5), $CaCl_2 \cdot 2H_2O$ (0.01), Na_2MoO_4 (0.01), $CoCl_2 \cdot 6H_2O$ (0.2), $AlK(SO_4)_2$ (0.01), $MgCl \cdot 6H_2O$ (0.2), $FeCl_3$ (0.1), $CuCl_2 \cdot 6H_2O$ (0.05). The composition of vitamin solution was as follows (concentration, g/L): riboflavin (0.025), citric acid (0.02), folic acid (0.01) and para–amino benzoic acid (0.01). The initial pH of the medium was adjusted to 6.7 using 1 M NaOH. Prior to inoculation, the medium was flushed with pure nitrogen (99.99%) for 15 min, sealed with rubber stoppers, crimped and autoclaved for 15 min at 121°C and 15 psi. Further, 10% v/v inoculum was added to the serum bottles, and the fermentation mixture was incubated at 36°C and 150 rpm. All experiments were carried out in duplicate. Aliquots of fermentation broth were withdrawn periodically for assessment of residual glycerol and other metabolites. Similarly, samples of gas phase products (accumulated above fermentation mixture) were collected periodically to quantify H_2 and CO_2 content.

2.2 Ultrasound–assisted glycerol fermentation

Ultrasound–assisted glycerol fermentation was carried out in an ultrasound bath (Make: Elma, Germany; Model: Transsonic T–460, Capacity: 2 L; Frequency: 35 kHz; Rated power input: 35 W). The bath was filled with water which acted as medium for propagation of ultrasound. Fermentation experiments were carried out in a 100 mL serum bottle with 50 mL working volume. The composition of the fermentation mixture was same as stated earlier. The serum bottle was placed at the center of the ultrasound bath and the flask was immersed in about 50% of its height in the water (Bhasarkar et al., 2015a; Khanna et al., 2012b; Singh et al., 2015b). The temperature of the water in the bath was maintained at 36°±2°C by circulating water bath. Sonication was applied in the duty cycle of 20% (i.e. 2 min ON and 8 min OFF in every 10 min of treatment). Prior to fermentation experiments, the ultrasound bath was characterized for acoustic power dissipation. Using calorimetric techniques, the amplitude of the ultrasound waves generated in the bath was determined as 1.5 bar.

2.3. In silico model construction and MFA

The *in silico* metabolic network of *C. pasteurianum* was constructed from experimental results, KEGG database of metabolic pathways (http://www.genome.jp/keg), and data reported in previous literature. The metabolic network was constructed with 26 reactions and 21 intracellular metabolites. Cellular composition of microbial culture *C. pasteurianum* MTCC 116 (ATCC 6013) used in present study was assumed to be the same as other Clostridial species reported in the literature (Cai et al., 2010; Jiang et al., 2013; Papoutsakis, 1984). Biomass formation (growth flux) was included into the model to account for the drain of intermediate metabolites into biomass. Metabolic fluxes of *C. pasteurianum* during glycerol fermentation were analyzed on the basis of glycerol metabolic pathway, with comparative assessment of numerical and experimental results. The specific rates of glycerol uptake and production of four metabolites, viz. acetate, butyrate, succinate and 1,3–PDO, were measured during the exponential phase of batch fermentation. The experimentally measured values of metabolite production were used as constraints in the *in silico* MFA. The specific hydrogen production rate was used as the criterion to evaluate the results, and to assess the concurrence between *in silico* MFA and experiments. The *in silico* MFA model used in this study was solved using MATLAB R2015a.

***Metabolic flux model*:** Metabolic flux analysis (MFA) is essentially a measure to determine steady–state reaction rates of different steps of substrate metabolism in microorganism. Input for the MFA is the stoichiometry matrix of intracellular metabolic reactions. MFA makes assumption of pseudo steady state for the intermediate metabolites, in which their net concentration at steady state is assumed to remain constant. The reaction rates or the metabolic fluxes are determined on the basis of molar balances of all intracellular metabolites. The boundary conditions for the analysis are experimentally measured values of the substrate consumption rate and formation rates of certain extracellular metabolites. The general

equation for MFA that relates intracellular metabolite concentrations, reaction fluxes, and the matrix of stoichiometric coefficients is written as:

$$dx/dt = S \cdot v \quad (1)$$

The above equation is essentially a dynamic mass balance equation for all metabolites. The LHS of above equation is m × 1 matrix of the time profiles of concentrations (x) of metabolites. The RHS has two matrices, viz. stoichiometric matrix S with dimensions m × r and reaction rate matrix v with dimensions r × 1. Element of the i^{th} row and j^{th} column in matrix S represents the stoichiometric coefficient of species i in reaction j. As per assumption of pseudo steady state, the intracellular concentrations (x) of all metabolites remain constant, and thus, equation 1 is written as:

$$S \cdot v = 0 \quad (2)$$

The degrees of freedom of the reaction system represented by eq. 2 is given as: $F = r - m$, where r = number of reactions, and m = number of intracellular metabolites. This necessitates that some of the elements in the matrix v are experimentally measured, so that remaining elements are determined by solving equation 2. In order to have unique solution of reaction system describe by eq. 2, experimental measurement of fluxes of F number of metabolites is needed. Manish et al., (2007) have suggested a simple procedure for determination of the remaining intracellular fluxes as follows:

The original vector v can be split into two components, viz. vector v_m that contains measured fluxes, and vector v_c containing the remaining fluxes. The original matrix of stoichiometric coefficient S can also be partitioned accordingly into two parts, viz. matrix S_m comprising of coefficients of measured reactions and matrix S_c containing the remaining reactions. Eq. (2) is then transformed as follows:

$$S_m.v_m + S_c.v_c = 0 \quad (3)$$

It may be noted that S_c is a square matrix (of dimensions m × m), as F (= $r - m$) number of fluxes are experimentally measured. Inversion of the S_c matrix yields the fluxes in vector v_c as follows:

$$v_c = -(S_c)^{-1}.S_m.v_m \quad (4)$$

The present system of glycerol metabolism comprises of 26 reactions with 21 metabolites. These reactions have been listed in Appendix A. Fig. 1 depicting the metabolic pathway of glycerol also shows the intermediate metabolites along with the metabolic reactions and the corresponding fluxes. The mass balance of all metabolites is depicted in Appendix B.

2.4 Analytical methods

The concentrations of metabolites in the samples withdrawn from fermentation broth were quantified by HPLC analysis using a Hi–Plex H column (300 mm × 8 µm × 7.7 mm, Agilent, India) thermostated at 60°C with the help of external column oven (Model: HCO–02, PCI analytics Pvt. Ltd., India). 0.01 M H_2SO_4 in ultra–pure water (18.2 MΩ·cm resistivity at 25°C) was used as the mobile phase at a flow rate of 0.5 mL/min. Residual glycerol content of the fermentation samples was quantified by HPLC analysis using a Rezex RCM Monosaccharide calcium–column (300 mm × 8 µm × 7.8 mm, Phenomenex, India) thermostated at 35°C with the help of external column oven (Model– HCO–02, PCI analytics Pvt. Ltd., India). Ultra–pure water (18.2 MΩ·cm resistivity at 25°C) was used as the mobile phase at a flow rate of 0.5 mL/min. The HPLC apparatus comprised of a pump (Series 200, Perkin Elmer), a refractive index detector (Series 200, Perkin Elmer) and a vacuum degasser (Series 200, Perkin Elmer). Reaction mixture samples were centrifuged (12,000 rpm, 20 min) and filtered through a 0.2 µm membrane filter, and diluted appropriately prior to injection into HPLC. Standard calibration plots were used to determine concentrations of the metabolites and glycerol in the samples of fermentation mixture.

The composition of product gas from glycerol fermentation was determined using Gas

Chromatograph (Make: Thermo scientific, Model: Ceres800 plus) with thermal conductivity detector (TCD) and Porapak Q (60/80 mesh) column employing argon as carrier gas at a flow rate of 30 mL/min. The operational temperature of the column oven was 45°C, and the injector and detector temperatures were maintained at 200°C. Gas samples were withdrawn from fermentation serum bottles and the molar/volumetric content of H_2 and CO_2 in the gas was determined. Hydrogen gas production was calculated from measurement of headspace of fermentation bottles (above surface of fermentation mixture). The total volume of gas produced in each time interval can be determined using the mass balance equation.

$$V_{H,i} = V_{H,i-1} + C_{H,i}\,(V_{G,i} - V_{G,i-1}) + V_H\,(C_{H,i} - C_{H,i-1}) \quad (5)$$

$V_{H,i}$ and $V_{H,i-1}$ are the cumulative hydrogen gas volumes at present (i) and previous (i–1) time interval, respectively; $V_{G,i}$ and $V_{G,i-1}$ are total product gas volume at the current and previous time intervals; $C_{H,i}$ and $C_{H,i-1}$ are the volume or mole fractions of hydrogen gas in the headspace at the current and previous time intervals; V_H is the volume of headspace of vials. The volume of product gas used for analysis was also taken into account during hydrogen mass balance.

3. Results and Discussion

3.1 Carbon mass balance for glycerol fermentation by *C. pasteurianum*

The carbon mass balance of glycerol fermentation by *C. pasteurianum* was examined by monitoring the time profiles of various metabolites such as CO_2, acetate, butyrate, succinate and 1,3–PDO for both control (mechanical shaking) and test (mechanical shaking with intermittent sonication) experiments. The carbon mass balance for control and test experiments is summarized in Table 1 and 2, respectively. It can be inferred from data presented in Tables 2 and 3 that butyrate and 1,3–PDO were the main intermediates of glycerol metabolism. This also implies that hydrogen production from glycerol metabolism in *C. pasteurianum* is mainly associated with formation of butyrate. In addition to acetate and

butyrate, the major fraction of carbon is distributed in the form of biomass or cell growth itself. Our previous results (Sarma et al., 2016) have shown that biomass growth and H_2 production are concurrent processes, which also supports the conclusion that biohydrogen is a cell growth associated product. Comparative analysis of Table 1 and 2 reveals marked influence of ultrasound in enhancing the glycerol metabolism. It could be observed that glycerol consumption rate increases by ~ 50% with application of sonication, as 80% of initial glycerol is consumed within 12 h in test experiments as against 18 h in control experiments. Nonetheless, production rates of all metabolites show non–uniform enhancement with sonication. The highest enhancement of > 70% is seen in production of succinate, followed by butyrate (> 50%). Production rate of 1,3–PDO, however, shows only marginal improvement of ~ 20% with sonication. Another significant influence of sonication on glycerol fermentation is in terms of carbon distribution to biomass formation. With application of sonication, the carbon distribution towards biomass growth drops by ~ 20%. Cai et al., (2010) and Cheng et al., (2013) have outlined the significance of butyrate to acetate ratio (B/A ratio) for H_2 production. Greater production of H_2 is favored by higher B/A ratio or higher butyrate yield. On the other hand, lactate formation has adverse effect on H_2 production due to lack of re–oxidation and consumption of NADH (Santilal et al., 2015). In the present study, the B/A ratio is found to increase with application of ultrasound. This is manifested in terms of ~40% rise in the H_2 yield (0.869 mol H_2/mol glycerol) in the test experiments as compared control experiments (0.622 mol H_2/mol glycerol). As per the glycerol metabolism reactions 1 and 2, the acetate route of glycerol metabolism yields 3 mol H_2/mol glycerol, while butyrate route of glycerol metabolism yields 2 mol H_2/mol glycerol. This stoichiometric relation points to reduction in H_2 yield with increasing B/A ratio. However, experimental results violate the stoichiometric prediction and show opposite trend of H_2 yield with B/A ratio. Two plausible explanations for this result have been given by Cheng et al., (2012) as follows:

(1) Consumption of acetate and lactate for production of butyrate and H_2 in anaerobic fermentation leading to higher H_2 yield at higher B/A ratio.

(2) H_2 and CO_2 or butyrate consumption for acetate production through acetogenesis resulting in lower H_2 yield at lower B/A ratio.

3.2 Metabolic flux analysis

The *in silico* metabolic network of *C. pasteurianum* was constructed using the reaction scheme given in Appendix A. Intracellular fluxes of *C. pasteurianum* in glycerol fermentation were determined using metabolic network and experimentally measured rates of formation/consumption of certain metabolites/substrates. As noted earlier, the specific rates of glycerol uptake and production rates of four metabolites, viz. acetate, butyrate, succinate and 1,3–PDO during exponential phase of fermentation have been experimentally measured. These rates form the constraints or boundary conditions for solving the pseudo–steady state metabolic flux balance given by eq. 6. The results of the metabolic flux analysis are shown in Table 3. It can be inferred from Table 3 that experimental (measured) and *in silico* (calculated by MFA model) results on specific H_2 production rate matched very well. The biomass formation equation was obtained from cellular composition of *C. butyricum* and *C. acetobutylicum*, as no detailed information about *C. pasteurianum* cells was available in published literature. The results of metabolic flux analysis are depicted in Fig. 1 for the control and test experiments. According to the MFA results shown in Fig. 1, the flux through the Embden–Meyerhof (EM) pathway is about five times as much as that through the pentose phosphate (PP) pathway. This indicates predominance of glycerol metabolism through EM pathway resulting in formation of pyruvate. Pyruvate is subsequently converted to lactate or acetyl–CoA with co–generation of reduced ferredoxin, from which hydrogen is formed directly by the action of hydrogenase. In order to get insight into the influence of ultrasound on carbon flux distribution in *C. pasteurianum*, MFA was performed under both control and

test experiments. As seen from Fig. 1, application of ultrasound influenced the metabolic fluxes at three key nodes, viz. PEP, pyruvate and acetyl–CoA. At the PEP node, the fraction of carbon flux towards pyruvate was higher as compared to the flux towards OAA. Marked increase of 47% in the metabolic flux towards OAA in test is a possible consequence of modifications in the secondary structure of PEP carboxylase enzyme due to intermittent sonication which increases its affinity towards the substrate PEP. At the pyruvate node, the fraction of carbon flux to acetyl–CoA and H_2 was higher as compared to the flux towards lactate. Smaller flux distribution towards lactate favors H_2 production, as confirmed by several previous authors (Cai et. al., 2010; Oh et al., 2007). With application of ultrasound, the fraction of carbon flux towards lactate increased by 84% from 1.02 to 1.88. However, this flux is still far less as compared to the sum total of fluxes (8.14) towards AcCoA and H_2. At the pyruvate node, three enzymes compete for pyruvate as substrate, viz. pyruvate:pyruvate ferredoxin oxidoreductase, pyruvate dehydrogenase and lactate dehydrogenase. The relative values of fluxes mentioned above indicate most flux is directed to reduced ferredoxin (FdH_2) and acetyl–CoA, both of which are associated with maximum H_2 production. It was also observed that, most of the flux from glycerol was directed towards 3–HPA formation, which is an immediate intermediate for 1,3–propanediol. This is in accordance with the experimental results, which have revealed 1,3 PDO to be the major product of glycerol metabolism (refer to Table 1 and 2).

Carbon flux distribution at the acetyl–CoA node was greatly affected by sonication as the flux towards butyrate increased by 133% in test experiments, whereas flux towards acetate increased by ~ 11%. The yields of major products from glycerol metabolism are shown in Table 4. The yield of biohydrogen showed marked rise (~ 40%) in test experiments. The MFA results indicate that enhancement in H_2 yield from ultrasound–assisted glycerol fermentation is

manifestation of enhanced flux towards butyrate. This conclusion is also corroborated by higher butyrate/acetate ratio in the test experiments as shown in Table 4.

3.3 Contemplations for enhancing H_2 production and their assessment with MFA

Despite enhancement in H_2 yield with application of ultrasound in glycerol fermentation, the yield of 0.869 mol H_2/mol glycerol obtained in present study is far lower than the H_2 yield from conventional processes such as catalytic steam reforming of glycerol (typical yield of ~ 6 mol H_2/mol glycerol). Several causes contribute to lowering of the H_2 yield in dark fermentation. One of the main causes leading to reduction in H_2 yield is accumulation of fermentation end products in fermentation broth which inhibit hydrogen production. The main metabolites of dark fermentation are acetic acid and butyric acid which leads to acidification of the fermentation broth. Reduction in pH of the fermentation broth initiates solventogenesis and results in lowering of the H_2 yield. The stoichiometry of glycerol fermentation (equation 2) suggests that hydrogen yield is 2 mole H_2 per mole of glycerol, when butyrate was the sole by–product. It was also found that butyrate had inhibitory effects on hydrogen production (Chin et al., 2003). The butyrate formation pathway is considered as the main competing pathway during H_2 production because it consumes more NADH than other pathways, reducing the yield of H_2 (Saint–Amas et al., 2001; Kumar et al., 2001; Hallenbeck et al., 2009). Despite these theoretical contemplations, experimental results presented in preceding sections have indicated increasing H_2 yield with butyrate/acetate ratio, and we have outlined some possible causes leading to this discrepancy. Nonetheless, it can also be conjectured that elimination of the butyrate pathway and the increased production of acetate may increase the H_2 yield per unit substrate consumption in *Clostridial* fermentation (Hallenbeck et al., 2009; Cai et al., 2011).

In this study, we have made assessment of two theoretical contemplations for further enhancement of H_2 yield (simultaneously with application of ultrasound) using the MFA model for glycerol metabolism by *C. pasteurianum*:

(i) Elimination of butyrate pathway in the *in silico* metabolic network of *Clostridium pasteurianum*: In this case, the flux from acetyl–CoA to butyrate, denoted as $v_{21,}$ was assumed to be nullified ($v_{21} = 0$) and the effect on H_2 flux was analysed by MFA. MFA analysis shown in Fig. 2 revealed that for $v_{21} = 0$, flux towards hydrogen (v_{20}) increased significantly. The increase in v_{20} was 37% in control experiments (employing mechanical shaking), and 62% in test experiments (employing sonication). The elimination of the butyrate pathway is possible *in vivo* by knockout of genes encoding the enzymes involved in the butyrate formation pathway, viz. β–hydroxy butyryl–CoA dehydrogenase (BHBD), 3–hydroxy–CoA dehydratase (CRT), butyryl–CoA–dehydrogenase (BCD), phosphotransbutyrylase (PTB), and butyrate kinase (BK).

(ii) Doubling the glycerol uptake rate in *C. pasteurianum*: The glycerol uptake rate can be enhanced *in vivo* by high–level expression of genes encoding enzymes involved in the *dha* (dihydroxyacetone) system composed of glycerol kinase (GK) and glycerol dehydrogenase (GDH). In this case, the flux from glycerol to DHAP (v_1) was assigned a value 2× the experimental value. This exercise was done for both test and control experiments. Results of MFA analysis depicted in Fig. 3 revealed that doubling the glycerol uptake rate enhances the flux towards H_2 approx. 2.5× times for both control and test experiments. These two theoretical approaches to enhance H_2 yield can provide valuable insights for construction of *C. pasteurianum* mutants lacking butyrate pathway or having over–expressed genes for higher glycerol uptake.

4 Conclusion

MFA of glycerol fermentation has provided insight into influence of ultrasound on intracellular carbon flux in *C. pasteurianum*. Glycerol uptake flux and butyrate flux at acetyl–CoA node showed increase of ~50% and ~133%, respectively, with sonication. ~40% increase in biohydrogen yield with sonication is accompanied by >65% rise in butyrate/acetate ratio. Thus, greater biohydrogen generation is attributed to higher carbon flux at acetyl–CoA node flowing to butyrate. Hypothetical MFA of ultrasound–assisted fermentation with nullifying of butyrate flux (or complete carbon partitioning to acetate at acetyl–CoA node) or doubling of glycerol uptake flux predicted further increase in biohydrogen yield.

Acknowledgements

The authors gratefully acknowledge valuable discussions and suggestions from Dr. Debasish Das and Dr. Soumen Kr. Maity (Department of Biosciences and Bioengineering, I.I.T. Guwahati). Authors are also grateful to Dr. S. Venkata Mohan (and his research group) in IICT Hyderabad for their valuable help and guidance in experimental work.

Supplementary material

The following supplementary material has been provided with the revised manuscript: (1) Table S.1: Summary of literature on metabolic flux analysis of biohydrogen production utilizing different substrates and microbial strains (2) Table S.2: Stoichiometric matrix S for MFA analysis

References

[1] Ahrens, K., Menzel, K., Zeng, A.P., Deckwer, W.D., 1997. Kinetic, Dynamic, and Pathway Studies of Glycerol Metabolism by *Klebsiella pneumoniae* in Anaerobic

Continuous Culture: III. Enzymes and Fluxes of Glycerol Dissimilation and 1,3–Propanediol Formation. Biotechnol. and Bioeng. 59, 544–552.

[2] Bhasarkar, J.B., Dikshit, P.K., Moholkar, V.S., 2015a. Ultrasound Assisted Biodesulfurization of Liquid Fuel using Free and Immobilized Cells of *Rhodococcus rhodochrous* MTCC 3552: A Mechanistic Investigation. Bioresour. Technol. 187, 369–378.

[3] Bhasarkar, J.B., Borah, A.J., Goswami, P., Moholkar, V.S., 2015b. Mechanistic analysis of ultrasound assisted enzymatic desulfurization of liquid fuels using horseradish peroxidase. Bioresour. Technol. 196, 88–98.

[4] Borah, A.J., Agarwal, M., Poudyal, M., Goyal, A., Moholkar, V.S., 2016. Mechanistic investigation in ultrasound induced enhancement of enzymatic hydrolysis of invasive biomass species. Bioresour. Technol. 213, 342–349.

[5] Chin, H., Chen, Z., Chou, C.P., 2003. Fedbatch operation using *Clostridium acetobutylicum* suspension culture as biocatalyst for enhancing hydrogen production. Biotechnol. Prog. 19, 383–388.

[6] Cai, G., Jin, B., Monis, P., Saint, C., 2011. Metabolic flux network and analysis of fermentative hydrogen production. Biotechnol. Advances. 29, 375–387.

[7] Ciranna, A., Pawar, S.S., Santala, V., Karp, M., van Niel, E.W.J., 2014. Assessment of metabolic flux distribution in the thermophilic hydrogen producer *Caloramator celer* as affected by external pH and hydrogen partial pressure. Microb. Cell. Fact. 13, 48.

[8] Dikshit, P.K., Moholkar, V.S., 2016. Kinetic analysis of dihydroxyacetone production from crude glycerol by immobilized cells of *Gluconobacter oxydans* MTCC 904. Bioresour. Technol. 216, 948–957.

[9] Ghimire, A., Frunzo, L., Pirozzi, F., Trably, E., Escudie, R., Lens, P.N.L., Esposito, G., 2015. A review on dark fermentative biohydrogen production from organic biomass: Process parameters and use of by–products. Applied Energ. 144, 73–95.

[10] Guo, X.M., Trably, E., Latrille, E., Carrere, H., Steyer, J.P., 2010. Hydrogen production from agricultural waste by dark fermentation: A review. Int. J. Hydrogen Energ. 35, 10660–10673.

[11] Hadicke, O., Grammel, H., Klamt, S., 2011. Metabolic network modelling of redox balancing and biohydrogen production in purple non sulfur bacteria. BMC Syst. Biol. 5, 150.

[12] Hallenbeck, P.C., 2009. Fermentative hydrogen production: principles, progress, and prognosis. Int. J. Hydrogen Energ. 34, 7379–7389.

[13] Jiang, L., Song, P., Zhu, L., Li, S., Hu, Y., Fu, N., Huang, H., 2013. Comparision of metabolic pathway for hydrogen production in wild type and mutant *Clostridium tyrobutyricum* starin based on metabolic flux analysis. Int. J. Hydrogen Energ. 38, 2176–2184.

[14] Jitrwung, R., Yargeau, V., 2011. Optimization of media composition for the production of biohydrogen from waste glycerol. Int. J. Hydrogen Energ. 36, 9602–9611.

[15] Khanna, S., Goyal, A., Moholkar, V.S., 2012a. Microbial conversion of glycerol: present status and future prospects. Crit. Rev. Biotechnol. 32, 235–262.

[16] Khanna, S., Jaiswal, S., Goyal, A., Moholkar, V.S., 2012b. Ultrasound enhanced bioconversion of glycerol by *Clostridium pasteurianum*: A mechanistic investigation. Chem. Eng. J. 200–202, 416–425.

[17] Khanna, S., Goyal, A., Moholkar, V.S., 2013a. Effect of fermentation parameters on bio–alcohols production from glycerol using immobilized *Clostridium pasteurianum*: an optimization study. Prep. Biochem. Biotechnol. 43, 828–847.

[18] Khanna, S., Goyal, A., Moholkar, V.S., 2013b. Production of n–butanol from biodiesel derived crude glycerol using *Clostridium pasteurianum* immobilized on amberlite. Fuel. 112, 557–561.

[19] Khanna, S., Goyal, A., Moholkar, V.S., 2013c. Mechanistic investigation of ultrasonic enhancement of glycerol bioconversion by immobilized *Clostridium pasteurianum* on silica support. Biotechnol. and Bioeng. 110, 1637–1645.

[20] Khanna, S., Shukla, A., Goyal, A., Moholkar, V.S., 2014. Alcoholic Biofuels production from biodiesel derived glycerol by *Clostridium pasteurianum* whole cells immobilized on silica. Waste and Biomass Valorization. 5, 789–798.

[21] Kumar, N., Ghosh, A., Das, D., 2001. Redirection of biochemical pathways for the enhancement of H_2 production by *Enterobacter cloacae*. Biotechnol. Lett. 23, 537–541.

[22] Liu, X., Ren, N., Song, F., Yang, C., Wamg, A., 2008. Recent advances in fermentative biohydrogen production. Progress in Natural Science 18, 253–258.

[23] Mangayil, R., Karp, M., Santala, V., 2012. Bioconversion of crude glycerol from biodiesel production to hydrogen. Int. J. Hydrogen Energ. 37, 12198–12204.

[24] Mangayil, R., Aho, T., Karp, M., Santala, V., 2015. Improved bioconversion of crude glycerol to hydrogen by statistical optimization of media components. Renew. Energ. 75, 583–589.

[25] Mathews, J., Wang, G., 2009. Metabolic pathway engineering for enhanced biohydrogen production. Int. J. Hydrogen Energ. 34, 7404–7416.

[26] Marone, A., Varrone, C., Fiocchetti, F., Giussani, B., Izzo, G., Mentuccia, L., Rosa, S., Signorini, A., 2015. Optimization of substrate composition for biohydrogen production from buffalo slurry co–fermented with cheese whey and crude glycerol, using microbial mixed culture. Int. J. Hydrogen Energ. 40, 209–218.

[27] Morimoto, K., Kimura, T., Sakka, K., Ohmiya, K., 2005. Overexpression of a hydrogenase gene in *Clostridium paraputrificum* to enhance hydrogen gas production. FEMS Microbiol. Lett. 246, 229–234.

[28] Mu, Y., Zheng, X–J, Yu, H–Q., 2009. Determining optimum conditions for hydrogen production from glucose by an anaerobic culture using response surface methodology (RSM). Int. J. Hydrogen Energ. 34, 7959–7963.

[29] Papoutsakis, E.T., 1984. Equations and calculations for fermentations of Butyric acid bacteria. Biotechnol. Bioeng. 26, 174–187.

[30] Saint–Amans, S., Girbal, L., Andrade, J., Ahrens, K., Soucaille, P., 2001. Regulation of carbon and electron flow in *Clostridium butyricum* VPI 3266 grown on glucose–glycerol mixtures . J. Bacteriol. 183, 1748–1754.

[31] Sarma, S., Dubey, V.K., Moholkar, V.S., 2016. Kinetic and thermodynamic analysis (with statistical optimization) of hydrogen production from crude glycerol using *Clostridium pasteurianum*. Int. J. Hydrogen Energ. 33, 1471–1482.

[32] Singh, S., Agarwal, M., Sarma, S., Goyal, A., Moholkar, V.S., 2015a. Mechanistic insight into ultrasound induced enhancement of simultaneous saccharification and fermentation of *Parthenium hysterophorus* for ethanol production. Ultrason. Sonochem. 26, 249–256.

[33] Singh, S., Sarma, S., Agarwal, M., Goyal, A., Moholkar, V.S., 2015b. Ultrasound enhanced ethanol production from *Parthenium hysterophorus*: A mechanistic investigation. Bioresour. Technol. 188, 287–294.

[34] Sittijunda, S., Reungsang, A., 2012. Biohydrogen production from waste glycerol and sludge by anaerobic mixed cultures. Int. J. Hydrogen Energ. 37, 13789–13796.

[35] Sridhar, J., Eiteman, M.A., 2001. Metabolic flux analysis of *Clostridium thermosuccinogenes*. Appl. Biochem. Biotechnol. 94, 51–69.

[36] Stephanopoulos, G.N., Aristidou, A.A., Nielsen, J., 2012. Metabolic Engineering–Principles and Methodologies, Academic Press, Diego, 1998 (Chapter 8: Metabolic flux analysis, pp. 313–350).

[37] Trchounian, K., Abrahamyan, V., Poladyan, A., Trchounian, A., 2015. *Escherichia coli* growth and hydrogen production in batch culture upon formate alone and with glycerol co–fermentation at different pH. Int. J. Hydrogen Energ. 40, 9935–9941.

[38] Urbaniec, K., Bakker, R.R., 2015. Biomass residues as raw material for dark hydrogen fermentation – A review. Int. J. Hydrogen Energ. 40, 3648–3658.

[39] Varrone, C., Giussani, B., Izzo, G., Massinim, G., Marone, A., Signorini, A., Wang, A., 2012. Statistical optimization of biohydrogen and ethanol production from crude glycerol by microbial mixed culture. Int. J. Hydrogen Energ. 37, 16479–16488.

[40] Wang, J., Wan, W., 2008. Optimization of fermentative hydrogen production process by response surface methodology. Int. J. Hydrogen Energ. 33, 6976–6984.

[41] Moholkar, V.S., Warmoeskerken, M. M. C. G., 2003.Integrated approach to optimization of an ultrasonic processor. AIChE J. 49(11), 2918–2932.

Table 1. Carbon mass balance for glycerol fermentation (control experiment with mechanical shaking) by *C. pasteurianum*

Time (h)	Glycerol (mg)	Acetate (mg)	Butyrate (mg)	1,3-PDO (mg)	Succinate (mg)	CO_2 (mg)	Biomass (mg)	Total carbon (mg)	Carbon balance (%)
0	370.00	0.	0.	0.	0.	0.	0.	370.00	100.00
3	291.50±0.01	2.75±0.02	15.53±0.12	39.58±0.33	2.59±0.11	1.55±1.20	16.57±0.01	370.06	100.02
6	232.75±0.13	5.34±0.13	20.92±0.32	44.30±0.23	3.14±0.22	6.54±1.11	32.12±0.01	345.11	93.27
9	199.67±0.11	7.04±0.11	22.17±0.15	58.69±0.06	3.25±0.02	13.80±0.96	54.17±0.55	358.79	96.97
12	147.36±0.32	8.76±0.18	29.47±0.16	59.98±0.17	3.45±0.21	20.69±0.98	74.54±0.19	344.23	93.04
15	112.01±0.01	7.50±0.11	32.78±0.02	62.01±0.11	3.43±0.06	33.83±1.23	85.53±0.04	337.08	91.10
18	74.01±0.50	9.01±0.01	40.12±0.04	69.76±0.02	3.36±0.07	35.12±0.99	92.24±0.01	323.61	87.46
24	65.35±0.40	8.88±0.01	44.32±0.50	68.13±0.30	3.33±0.35	33.21±1.01	104.25±0.11	327.26	88.45
Carbon distribution (%)	20.00	2.43	10.84	18.85	0.91	9.49	24.92		

Table 2. Carbon mass balance for glycerol fermentation (test experiment with ultrasound-irradiation) by *C. pasteurianum*

Time (h)	Glycerol (mg)	Acetate (mg)	Butyrate (mg)	1,3-PDO (mg)	Succinate (mg)	CO_2 (mg)	Biomass (mg)	Total carbon (mg)	Carbon balance (%)
0	370.	0.	0.	0.	0.	0.	0.	370.	100.
3	252.30±0.01	5.21±0.32	30.06±0.26	49.10±0.16	5.27±0.19	1.67±1.1	15.04±0.11	358.65	96.93
6	190.21±0.13	7.34±0.10	47.52±0.21	57.81±0.08	6.96±0.15	6.88±0.98	36.12±0.03	352.84	95.36
9	108.01±0.11	7.04±0.02	62.42±0.06	85.17±0.11	5.80±0.12	15.78±2.1	52.13±0.06	336.35	89.91
12	75.12±0.03	7.82±0.05	62.91±0.11	86.01±0.30	5.70±0.02	34.12±2.3	73.12±0.03	344.80	83.19
Carbon distribution (%)	20.3	2.11	17.00	22.24	1.54	9.22	19.76		

Table 3. Experimental metabolic rates and constraints used in *in silico* MFA

	Component	Control (Mechanical shaking)		Test (Ultrasound assisted)	
		Measured	Calculated	Measured	Calculated
Specific uptake rate (mmol/L/h)	Glycerol	3.50	--	5.80	--
Specific production rate (mmol/L/h)	Acetate	0.17	--	0.18	--
	Butyrate	0.51	--	1.19	--
	1,3-PDO	1.02	--	1.88	--
	Succinate	0.03	--	0.08	--
	H_2	2.70	2.80	3.85	4.07
H_2 yield (mol/mol glycerol)		0.63	0.70	0.89	0.95
Specific growth rate (h^{-1})		0.10	0.17	0.12	0.26

Table 4. Product yields under different operational conditions (Control: Mechanical shaking, Test: Ultrasound assisted)

	Product yields (mol/mol glycerol)						Butyrate/Acetate
	Acetate	Butyrate	1,3-PDO	Succinate	CO_2	H_2	
Control	0.046	0.142	0.285	0.008	0.248	0.622	3.086
Test	0.041	0.216	0.312	0.015	0.242	0.869	5.268

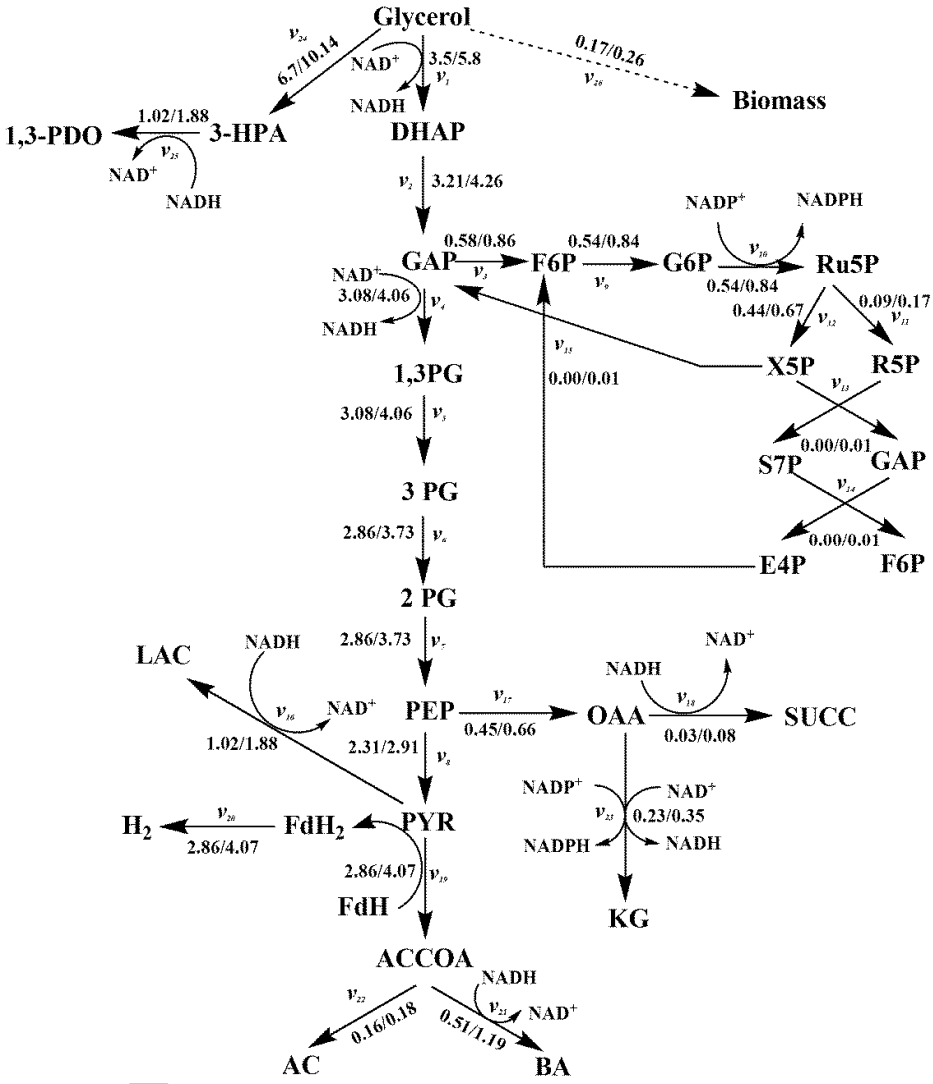

Figure 1. Metabolic flux distribution of hydrogen production pathway in *C. pasteurianum* with glycerol as the substrate in control (mechanical shaking)/test (mechanical shaking with intermittent ultrasound) experiments.

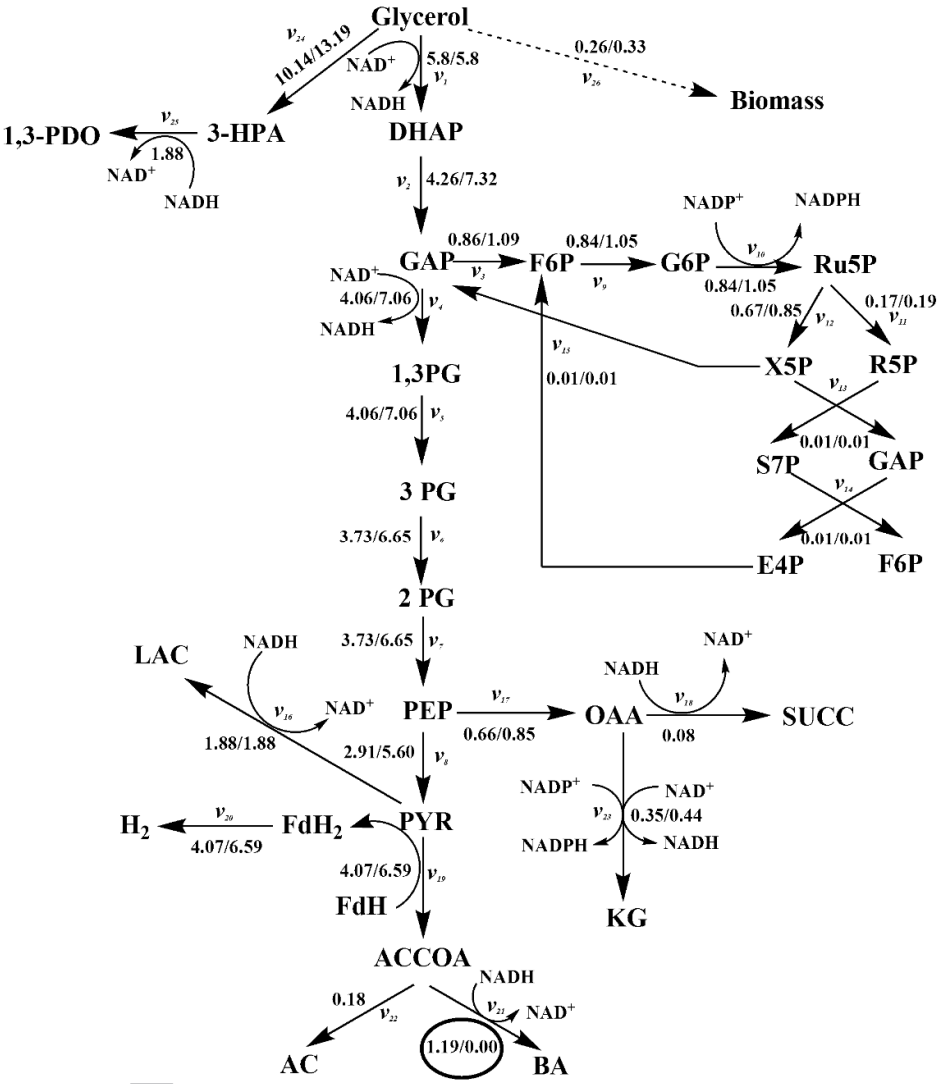

Figure 2. Metabolic flux distribution of hydrogen production pathway in *C. pasteurianum* with glycerol as the substrate when v_{21}=0 i.e. butyrate production assumed to be zero.

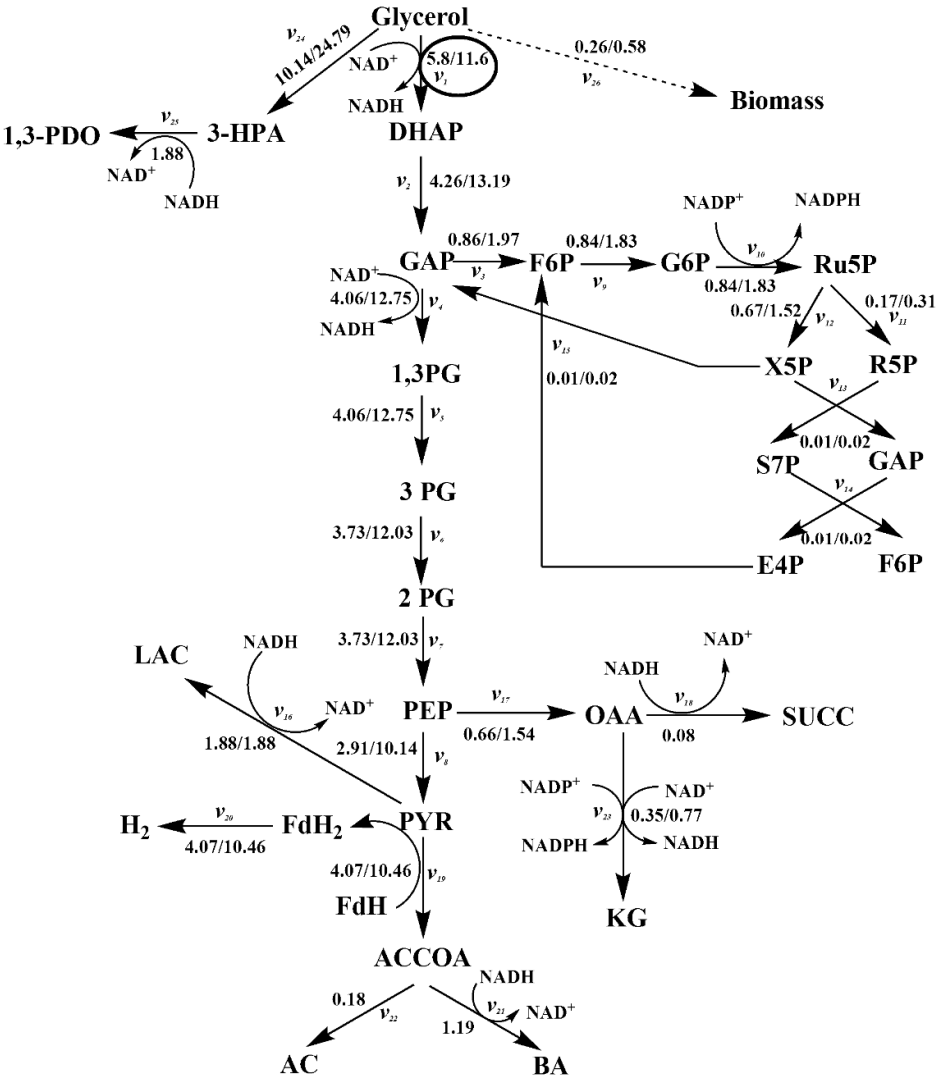

Figure 3. Metabolic flux distribution of hydrogen production pathway in *C. pasteurianum* with glycerol as the substrate when v_1=2x i.e. glycerol uptake rate is doubled.

RESEARCH HIGHLIGHTS

- Metabolic flux analysis of ultrasonic glycerol fermentation by *Clostridium pasteurianum.*
- Increase in H_2 yield by ~40%, glycerol uptake increase by >50%
- Greater partitioning of carbon flux at to butyrate Acetyl-CoA node
- Higher generation of H_2 accompanied by higher butyrate/acetate ratio
- Nullifying butyrate flux or doubling of glycerol uptake flux boosts H_2 production.